

# Perturbation-induced emergence of Poisson-like behavior in non-Poisson systems

Osman C Akin<sup>1</sup>, Paolo Paradisi<sup>2</sup> and Paolo Grigolini<sup>1,3,4</sup>

<sup>1</sup> Center for Nonlinear Science, University of North Texas, PO Box 311427, Denton, TX 76203-1427, USA

<sup>2</sup> Istituto di Scienze dell'Atmosfera e del Clima (ISAC-CNR), Lecce Unit, Strada Provinciale Lecce-Monteroni, km 1.2, 73100 Lecce, Italy

<sup>3</sup> Dipartimento di Fisica 'E Fermi'—University of Pisa, Largo Pontecorvo 3, 56127 Pisa, Italy

<sup>4</sup> Istituto dei Processi Chimico Fisici (IPCF-CNR), Area della Ricerca di Pisa, Via G Moruzzi 1, 56124 Pisa, Italy

E-mail: [ocakin@gmail.com](mailto:ocakin@gmail.com), [p.paradisi@isac.cnr.it](mailto:p.paradisi@isac.cnr.it) and [grigo@mail.df.unipi.it](mailto:grigo@mail.df.unipi.it)

**Abstract.** The response of a system with ON–OFF intermittency to an external harmonic perturbation is discussed. ON–OFF intermittency is described by means of a sequence of random events, i.e., the transitions from the ON to the OFF state and vice versa. The unperturbed waiting times (WTs) between two events are assumed to satisfy a renewal condition, i.e., the WTs are statistically independent random variables.

The response of a renewal model with non-Poisson ON–OFF intermittency, associated with non-exponential WT distribution, is analyzed by looking at the changes induced in the WT statistical distribution by the harmonic perturbation. The scaling properties are also studied by means of diffusion entropy analysis.

It is found that, in the range of fast and relatively strong perturbation, the non-Poisson system displays a Poisson-like behavior in both WT distribution and scaling. In particular, the histogram of perturbed WTs becomes a sequence of equally spaced peaks, with intensity decaying exponentially in time. Further, the diffusion entropy detects an ordinary scaling (related to normal diffusion) instead of the expected unperturbed anomalous scaling related to the inverse power-law decay.

Thus, an analysis based on the WT histogram and/or on scaling methods has to be considered with some care when dealing with perturbed intermittent systems.

**Keywords:** memory effects (theory), stochastic processes (theory), sequence analysis (theory)

---

## Contents

<b>1. Introduction</b>	<b>2</b>
<b>2. Renewal non-Poisson processes</b>	<b>4</b>
<b>3. Perturbation of the power index <math>\mu_0</math></b>	<b>7</b>
<b>4. Diffusion entropy analysis</b>	<b>11</b>
<b>5. Concluding remarks</b>	<b>13</b>
<b>Acknowledgments</b>	<b>14</b>
<b>References</b>	<b>14</b>

---

## 1. Introduction

Systems displaying ON–OFF intermittency are ubiquitous in Nature. The analysis of such systems is often carried out by means of a response to an external perturbation. An example of neurophysiological interest is given in the seminal work done by Moss and co-workers [1, 2]. These authors investigated the effect of an external harmonic perturbation on the dynamics of a neuron firing process, finding as the main effect that of reordering of the firings (or spikes) generated by the neuron dynamics. As a consequence, the histogram of inter-spike time distances or waiting times (WTs) becomes a sequence of equally spaced peaks, whose intensity decays with an exponential envelope. The time period of the peaks is equal to the period of the harmonic perturbation. The exponential envelope has been recently derived from the harmonic perturbation of a Poisson process [3], thereby suggesting that the experimental results of [1] and [2] may be an indication that neurons obey Poisson statistics. This is a quite intuitive result, as the unperturbed Poisson process is characterized by an exponential decay in the probability density function (PDF) of the WTs.

The exponential envelope of [1, 2] has been produced by the numerical and theoretical work of other authors. The work of [4] devotes great attention to the reset issue involved by the so called integrate–fire model [5]. The more recent work of [6] contains remarkably interesting analytical expressions for the inter-spike time distances (WTs) in the presence of harmonic perturbation.

It is interesting to note that results remarkably similar to those of the pioneering work of Moss and co-workers [1, 2] have been found [7] using the model of Fitzhugh and Nagumo [8]. The authors of [7] made a numerical calculation and found that the envelope

of the peaks in the inter-spike times histogram is indistinguishable from an exponential function.

Another model widely used to model firing neurons is the Hodgkin–Huxley neural model [9], which has been the subject of some recent studies aiming at establishing the response of this model to a harmonic perturbation [10]–[13]. Although there is controversy as regards whether or not a stochastic gain is obtained, the papers of [10]–[12] seem to recover the exponential envelope of Moss and co-workers [1, 2], which in turn is shown to be compatible with the assumption of Poisson statistics. The authors of [13], in contrast, reveal the emergence of an anomalous scaling.

Finally, in the work of Reibold *et al* [14] the authors recovered the exponential envelope of the pioneer work of Moss and co-workers [1, 2] from a theoretical picture adopting an intermittent map, which definitely departs from the Poisson condition.

According to some neurophysiologists, neurons follow renewal [15] and non-Poisson processes [16], i.e., the inter-event time distances (WTs) are mutually independent random variables with non-exponential PDF and the statistical distribution of the number of events in a given time interval is a non-Poisson distribution.

In summary, a crucial aspect resulting from this brief review is the possibility of observing the emergence of a Poisson-like behavior (exponential envelope in the WT histogram) by perturbing a system displaying anomalous scaling. The Poisson condition is not compatible with anomalous scaling, so an apparent contradiction seems to arise from these results.

In this paper this issue is investigated, considering that the Poisson-like behavior is surely related to the way the unperturbed non-Poisson statistics interacts with the external perturbation. The results are limited to the assumption that the unperturbed system generates WT sequences in agreement with a renewal non-Poisson random process [17]. In particular, it is assumed that the WTs generated by the unperturbed renewal non-Poisson process are distributed according to the following class of Pareto power-law PDFs:

$$\psi(\tau) = (\mu_0 - 1) \frac{T_0^{\mu_0 - 1}}{(\tau + T_0)^{\mu_0}}, \quad (1)$$

with

$$2 < \mu_0 < \infty; \quad T_0 > 0. \quad (2)$$

In this range of parameters the mean time is finite and given by

$$\langle \tau \rangle = \frac{T_0}{(\mu_0 - 2)}. \quad (3)$$

The choice of equation (1) is made to yield in the asymptotic time limit the inverse power law  $1/\tau^{\mu_0}$ , while making the WT distribution  $\psi(\tau)$  fulfil the normalization condition, without introducing any short-time truncation. The timescale  $T_0$  has the important role of defining the extension of the region of transition from the short-time condition, with no unphysical divergence, to the long-time limit, where the inverse power law appears. The power index  $\mu_0$  signals the specificity of the cooperative properties that establish the complex nature of the process.

Following the theoretical perspective of [18]–[21], the following sections are dedicated to introducing a model generating sequences of WTs distributed according to the

PDF of equation (1) and satisfying the renewal condition. According to this picture, the parameters  $\mu_0$  and  $T_0$  afford complete information about the unperturbed system dynamics, and it is a reasonable assumption that the effect of an external perturbing field is that of turning either  $T_0$  or  $\mu_0$ , or both, into time dependent parameters  $T(t)$  and  $\mu(t)$ . Here only the perturbation of the power index  $\mu_0$  is considered.

The outline of the paper is as follows. In section 2 a brief introduction to renewal non-Poisson processes with the Pareto WT PDF is given. In section 3 the effects of a harmonic perturbation on the power index  $\mu_0$  are discussed. In section 4 a concise review of the diffusion entropy (DE) method is given and some results on the scaling generated by a random walker associated with the perturbed WT sequences are shown. In section 5 some conclusions are drawn.

## 2. Renewal non-Poisson processes

A point process is described using a sequence of random times, at which some kind of crucial event occurs:  $\{t_i\}$ ,  $i = 0, 1, 2, \dots$ . The time instant  $t_0 = 0$  is the time of the first event occurrence. Denoting the WTs by  $\tau_{i+1} = t_{i+1} - t_i$ ,  $i = 0, 1, 2, \dots$ , the point process is defined to be renewal if the WTs  $\tau_i$  are mutually independent random variables [17]. In this approach, the spikes generated by neuron firings are critical events whose occurrence is associated with a mechanism erasing memory of the past. A renewal process is uniquely defined by the PDF of WTs (WT PDF)  $\psi(\tau_i)$ , which does not change with the index  $i$ . Equivalently, a renewal process is defined by the statistical distribution of the number of events in a given time interval. The non-exponential PDF of equation (1) corresponds to a non-Poisson distribution of the events. Another way of defining a renewal process is the local rate of event production  $r(t)$ . Roughly speaking, the local rate  $r(t)$  is the expected number of events per time unit in a neighborhood of the time  $t$ . More rigorously, following Cox [17] and assuming that the last event occurred at  $t_i$ , the local rate  $r(t)$  is the (conditional) probability density that an event occurs in an infinitesimal time interval  $[t, t + dt]$ , given that no events occurred in the time interval  $[t_i, t]$ :

$$r(t) = \lim_{dt \rightarrow 0} \frac{1}{dt} \Pr \{t < t_{i+1} \leq t + dt \mid t_{i+1} > t\}. \quad (4)$$

Considering the time interval between the first two events:  $[0, t_1]$ , it is easy to prove that the rate  $r(t)$  is given by [17]

$$r(t) = \frac{\psi(t)}{\Psi(t)} = -\frac{1}{\Psi(t)} \frac{d\Psi(t)}{dt}, \quad 0 < t < t_1, \quad (5)$$

with

$$\Psi(t) = \int_t^\infty \psi(s) ds = 1 - \int_0^t \psi(s) ds \quad (6)$$

being the survival probability, i.e., the probability that the WT is larger than  $t$ . Clearly, it results that  $\psi(t) = -d\Psi(t)/dt$ . Once the rate function  $r(t)$  is known, the survival probability is simply derived by solving equation (5) with respect to  $\Psi(t)$  and imposing the initial condition  $\Psi(0) = 1$ :

$$\Psi(t) = \exp \left( - \int^t r(t') dt' \right). \quad (7)$$

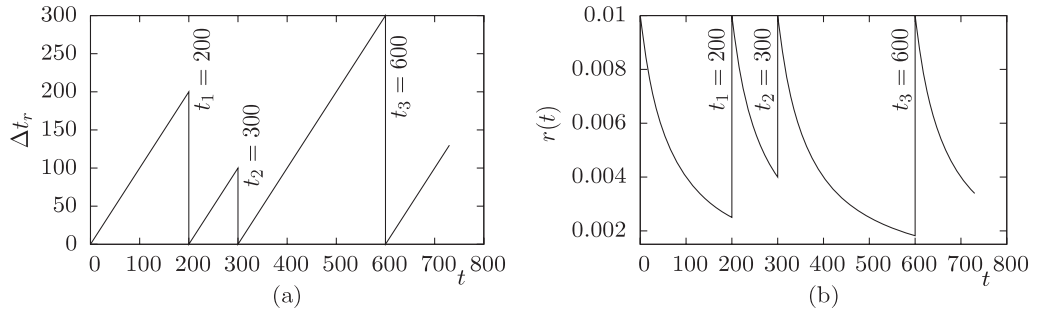


**Figure 1.** An example of the time evolution of (a) the renewal time function  $\Delta t_r$ , equation (15), and (b) the rate function  $r(t)$ , equation (16).  $r_0 = 0.01$ ,  $r_1 = 0.015$ .

The WT PDF in a Poisson process is given by an exponential decay and the associated event rate is constant in time:  $r(t) = r_0$  [17]. Consequently, a natural way to realize a non-Poisson process, and the relative non-exponential distribution of WT, is based on the assumption that the rate  $r(t)$  of event production changes in time. This is the case for Pareto's law, equation (1). In fact, in this case the survival probability is given by

$$\Psi(t) = \left( \frac{T_0}{t + T_0} \right)^{\mu_0 - 1}, \quad 0 \leq t < t_1. \quad (8)$$

Substituting in equation (5) and considering the time interval  $[0, t_1]$ , the following expression is obtained:

$$r(t) = \frac{r_0}{1 + r_1 t}, \quad 0 \leq t < t_1, \quad (9)$$

where

$$\mu_0 = 1 + \frac{r_0}{r_1}; \quad T_0 = \frac{1}{r_1} \quad (10)$$

and

$$r_0 = \frac{\mu_0 - 1}{T_0}; \quad r_1 = \frac{1}{T_0}. \quad (11)$$

The parameter  $r_0$  has the physical meaning of the rate value immediately after the occurrence of an event, whereas  $T_0 = 1/r_1$  determines the decay time of the rate function.

Note that the prescription of equation (9) applies only to the first time interval between the first firing at time  $t_0 = 0$  and the next one at time  $t = t_1 = \tau_1$ . To extend the rate function to the entire time axis, it is convenient to introduce the following auxiliary function:

$$f(t) = \frac{r_0}{1 + r_1 t}. \quad (12)$$

This corresponds to the rate function when no event occurs up to the absolute time  $t$ . Due to the renewal assumption, the occurrence of an event erases the system's memory and the rate function jumps from the value  $r(t_1) = f(t_1)$  to the 'initial' value  $r_0$ . An example of the behavior of the rate  $r(t)$  is displayed in figure 1(b), showing that the rate restarts

from the value  $r_0$  after each event, occurring at times  $t_1, t_2, t_3$ , etc. Consequently, in the time interval  $[t_1, t_2]$  the rate function is written in the following way:

$$r(t) = \frac{r_0}{1 + r_1(t - t_1)} = f(t - t_1), \quad t_1 \leq t < t_2. \quad (13)$$

For a given sequence of event occurrence times  $\{t_i\}$ , this expression is easily generalized by applying suitable time shifts to the basic rate function  $f(t)$ :

$$r(t) = f(t - t_i) = \frac{r_0}{1 + r_1(t - t_i)}, \quad t_i \leq t < t_{i+1}. \quad (14)$$

Rigorously, the rate function has a formal dependence on the sequence  $\{t_i\}$ :  $r(t, \{t_i\})$ . However, in contrast to the case for the absolute time  $t$ , the dependence on the sequence  $\{t_i\}$  is a kind of stochastic dependence, as the sequence of times is not known *a priori*, but it is a particular stochastic realization of the process, which is rigorously defined by the basic rate function  $f(t)$  given in equation (12). In the following the simple notation  $r(t)$  will be used, as its mathematical and physical meaning is unambiguous. Further, in order to lighten the notation when considering the external perturbation, it is appropriate to introduce the following *renewal time* function:

$$\Delta t_r(t, \{t_i\}) = t - t_i; \quad t_i \leq t < t_{i+1}. \quad (15)$$

The renewal time  $\Delta t_r$  is a kind of random time, which is set to zero when an event occurs, and it increases linearly in the absolute time  $t$  until the next event occurs. In particular, in the time interval  $[t_i, t_{i+1}]$ , it increases from 0 to  $\tau_{i+1} = t_{i+1} - t_i$ , which is exactly the random WT between the events labeled by the indices  $i$  and  $i + 1$  (see figure 1(a)). Using the renewal time function, the rate function of equation (14) is rewritten in the following way:

$$r(t) = \frac{r_0}{1 + r_1 \Delta t_r}, \quad (16)$$

where the dependence of  $\Delta t_r$  on  $t$  and  $\{t_i\}$  is left unindicated. From the computational point of view,  $\Delta t_r$  is simply the time measured from the last event.

Note that the renewal time function  $\Delta t_r$  describes the renewal character of the internal dynamics and its functional dependence on time  $t$  is not the sign of an external forcing. On the contrary, the time dependence of one or both the parameters  $r_0$  and  $r_1$  in equation (16) would be the sign of an external perturbation. Consequently, the more general mathematical prescription for an external perturbation can be written in the following general form:

$$r(t) = \frac{r_0 \phi_0(t)}{1 + r_1 \phi_1(t) \Delta t_r}. \quad (17)$$

In this formulation, the renewal character of the rate function  $r(t)$  is again included in  $\Delta t_r$ , which is affected by the occurrence of an event (see figure 1(a)), while the functions  $\phi_0(t)$  and  $\phi_1(t)$ , describing the effect of external forcings, are not affected by the internal critical events (e.g., neuron firings or spikes). By analogy with the unperturbed parameters  $\mu_0$  and  $T_0$  in equation (10), it is possible to write similar expressions for the perturbed power

index  $\mu(t)$  and the perturbed timescale  $T(t)$ :

$$\mu(t) = 1 + \frac{r_0\phi_0(t)}{r_1\phi_1(t)} = 1 + (\mu_0 - 1) \frac{\phi_0(t)}{\phi_1(t)}; \quad T(t) = \frac{1}{r_1\phi_1(t)} = \frac{T_0}{\phi_1(t)}. \quad (18)$$

The condition  $\phi_0(t) = \phi_1(t)$  has the effect of leaving the power index  $\mu_0$  unchanged, while affecting the timescale  $T_0$ . Making  $\phi_0(t)$  time dependent while keeping  $\phi_1(t) = 1$ , and thus time independent, has the effect of perturbing  $\mu_0$ , while leaving  $T_0$  unchanged.

A numerical algorithm, discrete in time, was used to generate the sequences of random times  $\{t_i\}$  corresponding to the rate  $r(t)$  of equation (17). This algorithm is based on an iterative procedure derived by the Cox definition of the rate of event production. In fact, considering the interval  $[t_i, t_{i+1}]$  and equation (4), the quantity  $p(t) = r(t) dt$  is the probability of an event occurrence in the infinitesimal interval  $[t, t + dt]$ , given that no events occurred in the interval  $[t_i, t]$ . In the implementation of a numerical scheme, the time step  $dt$  cannot be infinitesimal, but it is necessarily a finite quantity. In order to get a good approximation of the continuous-time model described by the rate given in equation (17), the time step  $dt$  must be chosen in such a way that (a)  $p_n = r(n \cdot dt + t_i) dt \ll 1$  for any value of  $t = n \cdot dt + t_i$  larger than  $t_i$  and (b)  $dt$  is much less than all the relevant timescales.

The resulting stochastic process, discrete in time, can be interpreted as a two-state Markov chain with jump probabilities  $p_n$  evolving in time. The quantity  $p_n$  is the probability of getting a jump at the discrete time  $n$ . The occurrence of an event corresponds to a jump between the two states and the residence time in each state defines the WT. Note that, if  $p_n$  is not very small, the two-state random process, discrete in time, is not a good approximation of the original model given in equation (17), even if  $p_n < 1$  (e.g.,  $p_n \sim 0.5$ ). This is also true when condition (a) is satisfied, but condition (b) is not. Considering the unperturbed rate  $r(t)$  of equation (16) and choosing  $dt = 1$ , from the conditions (a) and (b) it follows that

$$r_0 \ll 1; \quad r_1 \ll 1, \quad (19)$$

implying that the internal times  $1/r_0$  and  $T_0 = 1/r_1$  are much larger than the time step  $dt$ . These are the only two conditions required in the unperturbed case ( $\phi_0 \equiv \phi_1 \equiv 1$ ), but they must be completed with others involving the timescales of the external perturbation, included in the functions  $\phi_0(t)$  and  $\phi_1(t)$  of equation (17).

Note that the Poisson case is recovered by considering the unperturbed rate, equation (16), with  $r_1 = 0$ , implying  $r(t) = r_0$ , which is approximated by a two-state Markov chain with constant jump probability:  $p_n = r_0 dt = r_0$  ( $dt = 1$ ). As is known, the WT PDF is an exponential function with decay rate  $r_0$ .

### 3. Perturbation of the power index $\mu_0$

In this section the perturbation of  $r_0$  is considered, which, as proved by equations (10) and (18), is equivalent to perturbing the power index  $\mu_0$ , while leaving the timescale  $T_0$  unchanged. This is the straight generalization of the way of perturbing a Poisson process [3]. In fact, in the Poisson case  $r_1 = 0$ , so both  $\mu_0$  and  $T_0$  become infinite. The constant rate  $r(t) = r_0$ , being an inverse timescale, is the only basic parameter of the unperturbed Poisson process.

The perturbation of a Poisson process introduced in [3] is given by

$$r_p(t) = r_0 \exp \left[ \epsilon \cos \left( \frac{2\pi}{T_\omega} t \right) \right], \quad (20)$$

where  $r_p(t)$  denotes the perturbed Poisson rate, i.e., the perturbation of  $r_0$ , and  $T_\omega$  is the perturbation period. This is the same expression as is given in [2, 26] for the rate of escape (from each stable state) of a particle moving in a symmetric double-well potential under the effect of a white noise with intensity  $D$  and a harmonic signal with amplitude  $A$  and period  $T_\omega$ . The unperturbed rate  $r_0$  is then given by the Kramer formula:  $r_0 = C \exp(-Q/D)$ , where  $C$  is a constant depending on the frequency of the processes of molecular collision and  $Q$  is the potential barrier. The perturbation strength is given by  $\epsilon = Ax_m/D$  [2], where  $\pm x_m$  are the positions of potential minima, i.e., the stable points. The parameter  $D$  is not known from the experiments, and a range of  $D$  was selected by the authors of [2] in such a way as to get a good agreement between the double-well potential model and the experimental data. The corresponding range for  $\epsilon$  spans from about 4 to about 15.

It is straightforward to generalize the perturbation of the Poisson rate of equation (20) by considering it as a limit, for  $r_1 \rightarrow 0$ , of the non-Poisson rate given by equation (16), with  $r_p(t)$  replacing  $r_0$ . This is equivalent to perturbing the parameter  $r_0$  itself:

$$r(t) = \frac{r_p(t)}{1 + r_1 \Delta t_r} = \frac{r_0 \exp [\epsilon \cos((2\pi/T_\omega)t)]}{1 + r_1 \Delta t_r}, \quad (21)$$

and, as mentioned earlier, to perturbing the power index  $\mu_0$ . In fact, comparing with equation (17) it results that  $\phi_0(t) = \exp[\epsilon \cos((2\pi/T_\omega)t)]$  and  $\phi_1(t) = 1$  so, from equation (18), it is possible to write an expression for the power index, changing in time, associated with the rate given in equation (21):

$$\mu(t) = 1 + \frac{r_p(t)}{r_1} = 1 + [\mu_0 - 1] \exp \left[ \epsilon \cos \left( \frac{2\pi}{T_\omega} t \right) \right], \quad (22)$$

$\mu_0$  being given by equation (10).

From equation (21) it is possible to derive a linearized version of this model by simply using a Taylor expansion:

$$r(t) = \frac{r_0(1 + \epsilon \cos(2\pi t/T_\omega))}{1 + r_1 \Delta t_r}; \quad \epsilon < 1, \quad (23)$$

which implies for the power index

$$\mu(t) = \mu_0 + (\mu_0 - 1) \epsilon \cos \left( \frac{2\pi t}{T_\omega} \right); \quad \epsilon < 1. \quad (24)$$

Note that, setting in equation (20) the condition  $\epsilon \ll 1$ , the non-linear model of equation (21) becomes equivalent to the linear model of equation (23). Note that the linear and non-linear models are different. However, it is found from numerical simulations that these two models are significantly different only in the range  $\epsilon \sim 1$ .

The response of the renewal non-Poisson system to the external perturbation (both linear and non-linear) is determined by four parameters: the intensity  $\epsilon$  and the period  $T_\omega$  of the perturbation, the power index  $\mu_0$  and the timescale  $T_0$  of the unperturbed system.



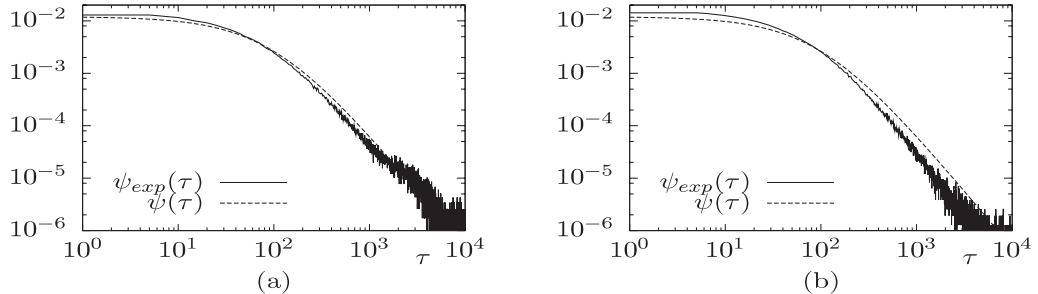


**Figure 2.** Slow linear perturbation of  $\mu_0$ , equation (23). Comparison of the perturbed histograms of the WTs,  $\psi_{exp}(\tau)$ , with the unperturbed ones,  $\psi(\tau)$ .  $\mu_0 = 2.2$ ,  $T_0 = 100$ ,  $\epsilon = 0.6$  (a)  $T_\omega = 5 \times 10^3$  ( $R = 10$ ); (b)  $T_\omega = 5 \times 10^6$  ( $R = 10^4$ ).

Note that a non-Poisson condition with  $\mu_0 > 2$  is considered, a condition ensuring that the mean value of  $\tau$  exists (see equation (3)). Therefore, following [3], it is possible to define the following dimensionless parameter:

$$R = \frac{T_\omega}{\langle \tau \rangle}. \quad (25)$$

When  $R \ll 1$ , the perturbation is faster than the production of firing events, thereby producing what it is defined as *fast perturbation*, linear or non-linear. The opposite limit,  $R \gg 1$ , is referred to as *slow perturbation*, linear or non-linear. Note that, as stated in section 2, the conditions of equation (19) must be supplemented with the following one:  $dt/T_\omega = 1/T_\omega \ll 1$ , associated with the timescale  $T_\omega$  of the external perturbation.

In the case of non-linear perturbation of  $\mu_0$ , the fast condition allows us to define the effective power index  $\mu_{eff}$  as follows:

$$\mu_{eff} = 1 + [\mu_0 - 1] \left\langle \exp \left[ \epsilon \cos \left( \frac{2\pi}{T_\omega} t \right) \right] \right\rangle, \quad (26)$$

where  $\langle \dots \rangle$  indicates an average over one perturbation period  $T_\omega$ . This average value is well defined only in the range of fast perturbation ( $R \ll 1$ ). In fact, when the condition  $R \ll 1$  applies, the perturbation makes  $\mu(t)$  execute many oscillations before reaching the time regime where  $\psi(\tau)$  reveals its inverse power-law nature. It is easy to prove that the average value  $\mu_{eff}$  is independent of the perturbation period  $T_\omega$ , but increases rapidly with the perturbation strength  $\epsilon$ . As the limit  $\mu_0 = \infty$  is associated with a genuine Poisson process, it is expected that very large values of  $\mu_{eff}$  could generate a Poisson-like behavior in the perturbed system, at least in the range of validity of equation (26). Conversely, it is also easy to see that the linear perturbation of  $\mu_0$ , given by equations (23) and (24), does not affect the effective power index, i.e.,  $\mu_{eff} = \mu_0$ . In section 4 the consequences of this behavior for the scaling properties detected by the DE analysis will be discussed in more detail.

Figures 2 and 3 display the main results obtained from the application of the numerical algorithm introduced in section 2 to the rate function of equations (21) and (23). Figures 2 and 3(a) refer to the linear perturbation of  $\mu_0$ , equation (23), with perturbation strength  $\epsilon = 0.6$ , and figure 3(b) is generated by the non-linear perturbation of  $\mu_0$ , equation (21),

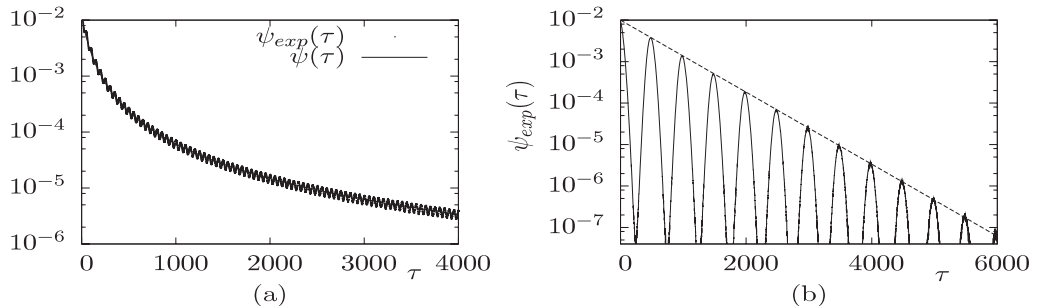


**Figure 3.** Fast perturbation of  $\mu_0$ . (a) Linear model, equation (23): comparison of the perturbed histogram of WT's (oscillating pattern  $\psi_{\text{exp}}(\tau)$ ) with the unperturbed one ( $T_0 = 100$ ,  $T_\omega = 50$ ,  $\mu_0 = 2.2$ ,  $R = 0.1$ ,  $\epsilon = 0.6$ ). (b) Non-linear model, equation (21): histogram of WT's ( $T_0 = 10^5$ ,  $T_\omega = 500$  ( $R = 10^{-3}$ ),  $\mu_0 = 2.2$ ,  $\epsilon = 7$ ). The dashed line in panel (b) is the exponential envelope of the maxima.

with strength  $\epsilon = 7$ , which is a value in agreement with the range used in [2]. The probability density of WT is only weakly affected by making perturbation very slow, namely,  $R \gg 1$ , as shown by the histograms reported in figure 2. The experimentally observed histogram, indicated with  $\psi_{\text{exp}}(\tau)$  and affected by the perturbation, is compared with the unperturbed histogram  $\psi(\tau)$ . In figure 3(a) a fast perturbation with the same strength  $\epsilon$  as for figure 2 is shown. In this case the fast perturbation produces more significant effects, as weak oscillations appears in the histogram. However, the weak oscillations of figure 3(a) do not affect the inverse power-law nature of  $\psi(\tau)$ , insofar as the histogram is clearly the addition of a genuinely power-law decay and of a pattern of weak and fast oscillations, with time period  $T_\omega$ . In conclusion, the histogram averaged over the time  $T_\omega$  results in a power-law decay with index  $\mu_0$ .

In figure 3(b) there is reported the WT histogram for the case of a fast and strong ( $\epsilon = 7$ ) non-linear perturbation of  $\mu_0$ , determining the emergence of a Poisson-like behavior, as is easily seen from the exponential envelope of the histogram maxima. Moving from the weak linear perturbation of figure 3(a) ( $\epsilon = 0.6$ ) to the strong non-linear perturbation of figure 3(b) ( $\epsilon = 7$ ), both fast, the non-exponential (power-law) average over the fast oscillation turns into a sequence of equally spaced peaks, displaying exponential decay of the intensities (exponential envelope). Further, the time distance between two peaks corresponds to the perturbation period. The exponential envelope of peak intensities is a property shared by the perturbed Poisson system of the earlier work of [3]. As mentioned earlier, this is why, at first sight, the result of figure 3(b), and the experimental results of [1, 2] as well, can be interpreted as the consequence of the harmonic perturbation of a Poisson process [3].

In summary, the numerical simulations showed that, on increasing the coupling strength  $\epsilon$ , the power-law decay emerges at a larger and larger timescale and the exponential envelope becomes more extended in time. On the other hand, the long WT's are rare, and in the histograms realized with sequences of finite size, the statistical errors of the long-time tails are so large as to make the presence of an inverse power-law behavior virtually invisible. This explains the lack of a significant deviation from the exponential behavior in figure 3(b) and the surprising qualitative similarity between the theoretical

distribution of figure 3(b) and the experimental distribution of figure 1(a) of [1] and figures 5 and 8 of [2]. As far as figure 3(b) is concerned, the origin of the exponential behavior rests on the fact, accounted for by equation (26), that the perturbation creates an effective  $\mu_{\text{eff}}$  of the order of 200.

In conclusion, the numerical results illustrated in this section show that a non-Poisson system under the influence of a strong and fast perturbation of the power index  $\mu_0$  may produce the exponential envelope of [1, 2].

#### 4. Diffusion entropy analysis

In this section the approach of [13] is used. The authors of [13] adopted the method of diffusion entropy (DE) [22]–[24] to analyze the data produced by the Hodgkin–Huxley (HH) neuron model.

The DE method rests on converting a time series into a diffusion process  $x(t)$ , and in evaluating the entropy of the resulting probability density function (PDF)  $p(x, t)$ . When the diffusion process is continuous in time and space, the diffusion entropy is defined in the following way:

$$S(t) = - \int_{-\infty}^{\infty} dx p(x, t) \ln(p(x, t)). \quad (27)$$

When the PDF  $p(x, t)$  satisfies the scaling condition:

$$p(x, t) = \frac{1}{t^\delta} F\left(\frac{x}{t^\delta}\right), \quad (28)$$

with exponent  $\delta$  defining the scaling, it is easy to prove that the DE satisfies the following general expression:

$$S(t) = A + \delta \ln(t), \quad (29)$$

where

$$A = - \int_{-\infty}^{\infty} dz F(z) \ln(F(z)). \quad (30)$$

According to [22] the efficiency of this method of analysis depends on the walking rule adopted to generate the diffusion process  $x(t)$ . In the following, the sequence of WTs is converted into a diffusion process with the asymmetric jump model (AJM) rule [22]. According to the authors of [22], the AJM walking rule is the most accurate one, and it leads to a fast convergence to the scaling condition.

With this rule each WT  $\tau$  is represented by a sequence of zeros, and then by a jump of constant length, say 1, in a fixed (positive) direction. The coordinate of the random walker  $x(t)$  is then defined as the sum of jumps that occurred up to time  $t$ . A general result is known in the case of a sequence of WTs whose probability density satisfies the asymptotic behavior:  $\psi(\tau) \sim 1/\tau^{\mu_0}$ , namely, the asymptotic behavior of the prescription of equation (1). In this case, the relation between the (unperturbed) scaling  $\delta_0$  of the AJM rule and the power index  $\mu_0$  is given by [22]

$$\delta_0 = \begin{cases} \frac{1}{\mu_0 - 1}; & 2 < \mu_0 < 3, \\ 0.5; & \mu_0 \geq 3. \end{cases} \quad (31)$$

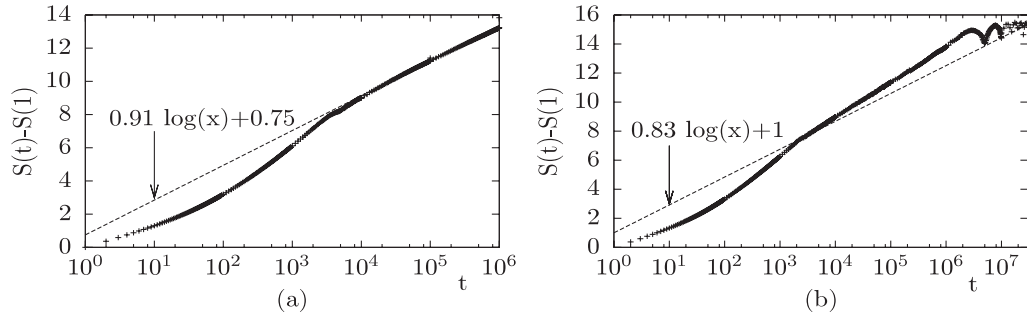


**Figure 4.** Slow linear perturbation of  $\mu_0$ , equation (23). Diffusion entropy (same parameters as for figure 2). Unperturbed scaling  $\delta_0 \simeq 0.83$ .

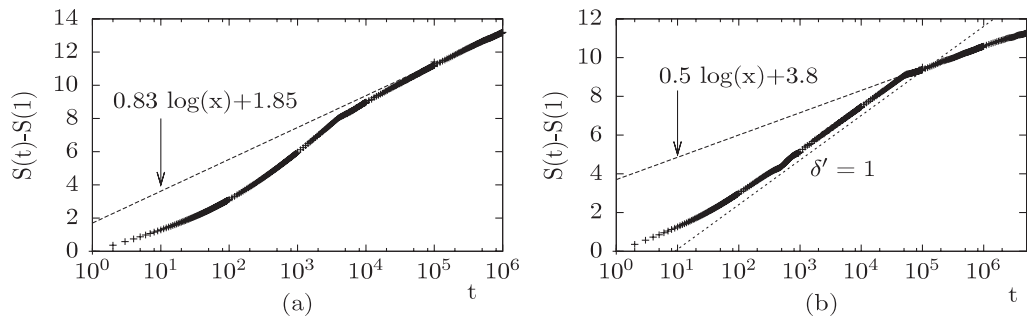


**Figure 5.** Fast perturbation of  $\mu_0$ , diffusion entropy (unperturbed scaling  $\delta_0 \simeq 0.83$ ). (a) Linear model, equation (23): same parameters as for figure 3(a). (b) Non-linear model, equation (21): same parameters as for figure 3(b).

Considering the unperturbed system, the transition from  $\mu_0 < 3$  to  $\mu_0 > 3$  corresponds to a transition where the scaling  $\delta_0$  is anomalous ( $\delta_0 > 0.5$ ) to the ordinary scaling  $\delta_0 = 0.5$  of normal diffusion. The Poisson condition corresponds to  $\mu_0 = \infty$ . However, for the Poisson scaling  $\delta_0 = 0.5$  to show up it is enough to cross the border  $\mu_0 = 3$ . For simplicity, the range  $\mu_0 < 3$  is defined as the non-Poisson basin and  $\mu_0 > 3$  as the Poisson basin. Thus, the adopting of the DE analysis allows one to establish whether the system is located in the Poisson or the non-Poisson basin through the measurement of  $\delta_0$ . Equation (31) applies also in the perturbed case. The perturbed scaling is denoted by  $\delta$ . If  $\delta > 0.5$  the system lives in the non-Poisson basin. The transition from  $\delta > 0.5$  to  $\delta = 0.5$  corresponds to a transition from the non-Poisson to the Poisson basin. Our guess is that the perturbed scaling  $\delta$  is related to the effective power index  $\mu_{\text{eff}}$  of equation (26) (at least in the fast perturbation case).

In figures 4 and 5 some results of DE analysis are shown. Figures 4 and 5(a) illustrate the DE analysis applied to the case of linear perturbation of  $\mu_0$ , as described by equation (23); figure 5(b) illustrates the DE analysis applied to the case of non-linear perturbation of  $\mu_0$ , according to the prescription of equation (21). Figures 4 and 5(a) correspond to the WT distributions of figures 2 and 3(a), respectively. Figure 4 shows the DE analysis applied to two distinct sequences, simulating the effect of two slow ( $R > 1$ ) linear perturbations of  $\mu_0$ . By comparing panels (a) and (b) of figure 4 and figure 5(a), it is possible to see that, in contrast to the case for the probability density, a clear oscillating

pattern emerges in the DE curve only in the case of very slow linear perturbation,  $R = 10^4$  (figure 4(b)). Figure 4(a) illustrates the case where the linear perturbation is moderately slow, namely, in between the fast condition of figure 5(a) and the very slow perturbation of figure 4(b).

First of all, according to the rule of equation (31), the power index  $\mu_0 = 2.2$ , shared by figures 4 and 5(a), is expected to yield  $\delta_0 \simeq 0.83$ .

For perturbation speeds ranging from the fast perturbation of figure 5(a) ( $R = 0.1$ ) to the intermediate perturbation of figure 4(a) ( $R = 10$ ), DE does not produce any significant sign of oscillating behavior, so in both cases a neat asymptotic scaling  $\delta$  appears. In the fast perturbation case (figure 5(a)) this scaling coincides with the unperturbed scaling  $\delta_0 \simeq 0.83$ , while in the intermediate case of figure 4(a) the scaling takes the value  $\delta = 0.91$ , significantly larger than  $\delta_0$ . In the case of very slow perturbation of figure 4(b) the unperturbed scaling  $\delta_0$  appears again, although as the slope of the straight line on which the relative minima of  $S(t)$  are located.

In the case of fast linear perturbation of figure 5(a), the time dependent power index  $\mu(t)$  of equation (24) oscillates many times within the timescale  $\langle\tau\rangle$ , so the DE analysis perceives only its time average  $\mu_{\text{eff}}$ , which, for the linear model of equation (23), is identical to  $\mu_0$ , thereby yielding the unperturbed scaling  $\delta_0$ . In the case of very slow perturbation of figure 4(b) we have to recall that the DE analysis rests on converting a single sequence into many diffusion trajectories using the mobile window method. When the length of the mobile window is equal to  $nT_\omega$ , the influence of external perturbation is annihilated. This is the same explanation as was used in [3] and in the references to DE analysis therein. As a consequence, the relative minima of  $S(t)$ , represented in the linear-log representation, lie on the straight line whose slope corresponds to the unperturbed scaling  $\delta_0$ .

In the intermediate range  $R \sim 10$  ( $T_\omega \sim 10\langle\tau\rangle$ ), displayed in figure 4(a), the scaling changes to the value  $\delta = 0.91$ , significantly larger than the unperturbed scaling  $\delta_0 = 0.83$ . This result suggests the emergence of a form of complexity which is the consequence of the joint action of non-Poisson statistics and harmonic perturbation.

Figure 5(b) illustrates the result of DE analysis in the case of fast non-linear perturbation of  $\mu_0$ , equation (21), which produces the WT distribution of figure 3(b).

An extended transition regime with the effective scaling of  $\delta' = 1$  exists, but, after this extended transient of the order of  $T_0$ , the emergence of an ordinary scaling  $\delta = 0.5$  rather than the unperturbed scaling  $\delta_0 \simeq 0.83$  is observed. According to the prescription of equation (31), the scaling  $\delta = 0.5$  corresponds to the condition  $\mu_0 > 3$ . A quite plausible explanation is that the DE analysis is mostly affected by the extended time intervals in which the effective power index  $\mu(t)$ , given in equation (22), is greater than 3. This is confirmed by the large value of the average power index  $\mu_{\text{eff}} \simeq 200$ , obtained by considering equation (26) with the parameters of figure 5(b).

## 5. Concluding remarks

The research work of this paper has been motivated by the experimental results of [1, 2]. In spite of this, the results are of general interest, providing some qualitative indications on the response of non-Poisson processes to external harmonic perturbations. In particular, the emergence of the exponential envelope in perturbed systems with non-Poisson statistics has been studied, limiting the investigation to the case of systems which are

renewal ones in the unperturbed state (but not necessarily when the perturbation is switched on). It has been shown that the phenomenon of an exponential envelope can emerge as the response to harmonic perturbations of both Poisson [3] and non-Poisson systems. In particular, the following results are found.

Result 1. A fast and relatively strong perturbation of  $\mu_0$ , equations (21) and (22), generates the exponential envelope in the histogram of waiting times and ordinary scaling of normal diffusion  $\delta = 0.5$ , even when the unperturbed system generates anomalous diffusion. This could be interpreted as a genuine transition from non-Poisson to Poisson statistics, associated with a transition from  $\mu_{\text{eff}} < 3$  to  $\mu_{\text{eff}} > 3$ . This is seen by substituting  $\mu_0$  with  $\mu_{\text{eff}}$  in equation (31). Note, however, that  $\mu_{\text{eff}}$  is well defined only in the case of fast perturbation (see equation (26)). The case of intermediate and slow perturbation deserves further investigation, as both equations (26) and (31) cease to be valid.

Result 2. A relatively weak harmonic perturbation of  $\mu_0$ , equations (23) and (24), either very slow or very fast, does not affect the system's complexity (i.e., the power index  $\mu_0$ ), which emerges again in the long-time region. However, in the intermediate range  $R \sim 10$  ( $T_\omega \sim 10\langle\tau\rangle$ ), a significant increase in the scaling parameter is observed (see figure 4(a)).

Consequently, some care must be taken in applying scaling methods to time series generated by intermittent systems perturbed with an external harmonic signal. Even a Poisson-like behavior in the histogram of waiting times (exponential envelope) is not necessarily the signature of the presence of Poisson statistics in the unperturbed system.

Further, it is important to underline that the condition  $\mu_{\text{eff}} > 3$  is a criterion identifying the emergence of Poisson-like behavior, at least in the fast perturbation regime. Unfortunately, this condition cannot be estimated explicitly from the experimental results found in the literature [1, 2], and even the regime of fast perturbation cannot be stated *a priori*. In fact, in our approach, this would require the knowledge of the internal parameters  $\mu_0$  and  $T_0$  (see equation (1)). This is also true for the models proposed in [1, 2, 26], where some model parameters, such as  $Q$ ,  $x_m$  and  $D$ , are not known (see comments after equation (20)). However, the results of this paper suggest that it should be appropriate to explore a more extended range of control parameters, i.e., the amplitude  $A$  and period  $T_\omega$  of the harmonic signal. Particular attention should be focused on the scaling detected by the diffusion entropy. By investigating the regime of small amplitudes, consistently with the limitations of the experimental setup, it could be possible for the perturbed system to fall within the range of relatively weak ( $\epsilon < 1$ ) perturbation. In this range, the Poisson-like behavior could disappear and some anomalous scaling could emerge (see, for example, figures 2(b) and 4(b)).

## Acknowledgments

OCA and PG gratefully acknowledge ARO for the financial support of this research through grant No. W911NF-05-1-0059. PP gratefully acknowledges financial support from Italian Government through grant 'CLIMESCO contract No. 285-20/02/2006'.

## References

- [1] Longtin A, Bulsara A and Moss F, 1991 *Phys. Rev. Lett.* **67** 656
- [2] Zhou T, Moss F and Jung P, 1990 *Phys. Rev. A* **42** 3161

- [3] Akin O C, Paradisi P and Grigolini P, 2006 *Physica A* **371** 157
- [4] Plesser H E and Geisel T, 2001 *Phys. Rev. E* **63** 031916
- [5] Lapique L, 1907 *J. Physiol.* **9** 620  
Tuckwell H C, 1989 *Stochastic Processes in the Neurosciences* (Philadelphia, PA: SIAM)  
Bulsara A R, Elston T C, Doering C R, Lowen S B and Lindenberg K, 1996 *Phys. Rev. E* **53** 3958  
Lánský P, 1997 *Phys. Rev. E* **55** 2040
- [6] Schindler M, Talkner P and Hänggi P, 2004 *Phys. Rev. Lett.* **93** 048102
- [7] Gong P-L and Xu J-X, 2001 *Phys. Rev. E* **63** 031906
- [8] Fitzhugh R, 1962 *Biological Engineering* ed H P Schwann (New York: McGraw-Hill)  
Nagumo J, Arimoto S and Yoshizawa S, 1962 *Proc. IRE* **50** 2061
- [9] Hodgkin A L and Huxley A F, 1952 *J. Physiol.* **117** 500
- [10] Liu F, Yu Y and Wang W, 2001 *Phys. Rev. E* **63** 051912
- [11] Khovanov I A and McClintock P V E, 2003 *Phys. Rev. E* **67** 043901
- [12] Chik D T W, Wang Y and Wang Z D, 2001 *Phys. Rev. E* **64** 021913
- [13] Yang H, Zhao F, Zhang W and Li Z, 2005 *Physica A* **347** 704
- [14] Reibold E, Just W, Becker J and Benner H, 1997 *Phys. Rev. Lett.* **78** 3101
- [15] van Vreeswijk C, 2001 *Neurocomputing* **38–40** 417
- [16] Baddeley R, Abbott L F, Booth M C A, Sengpiel F, Freeman T, Wakeman E A and Rolls E T, 1997  
*Proc. R. Soc. Lond. B* **264** 1775
- [17] Cox D R, 1967 *Renewal Theory* (New York: Chapman and Hall)
- [18] Bianco S, Grigolini P and Paradisi P, 2005 *J. Chem. Phys.* **123** 174704
- [19] Barbi F, Bologna M and Grigolini P, 2005 *Phys. Rev. Lett.* **95** 220601
- [20] Allegrini P, Ascolani G, Bologna M and Grigolini P, 2006 arXiv:cond-mat/0602281
- [21] Allegrini P, Bologna M, Grigolini P and West B J, 2007 *Phys. Rev. Lett.* **99** 010603
- [22] Grigolini P, Palatella L and Raffaelli G, 2001 *Fractals* **9** 439
- [23] Scafetta N, Hamilton P and Grigolini P, 2001 *Fractals* **9** 193
- [24] Grigolini P, Leddon D and Scafetta N, 2002 *Phys. Rev. E* **65** 046203
- [25] Parzen E, 1962 *Stochastic Processes* (San Francisco, CA: Holden-Day)  
Cox D R and Miller H D, 1965 *The Theory of Stochastic Processes* 1st edn (London: Chapman and Hall)
- [26] McNamara B and Wiesenfeld K, 1989 *Phys. Rev. A* **39** 4854